Assessment of Filmwise Wall Condensation Heat Transfer Models in SPACE Code Using Experimental Data and MARS-KS

Hyo Jun Ana, Jae Hyung Parka, Taeseok Kimb, JinHo Songa, Joon Eon Yanga, Sung Joong Kima,c*

^aDepartment of Nuclear Engineering, Hanyang University, 222 Wangsimnri-ro, Seongdong-gu, Seoul 04763, Republic of Korea

^bDepartment of Electrical Engineering, Jeju National University, 102 Jejudaehak-ro, Jeji-si, Jeju-do 63243, Republic of Korea

^cInstitute of Nano Science and Technology, Hanyang University, , 222 Wangsimnri-ro, Seongdong-gu, Seoul 04763, Republic of Korea

*Corresponding author: sungjkim@hanyang.ac.kr

*Keywords: SPACE code, Condensation experiment, V&V, Passive safety system.

1. Introduction

Condensation is one of the major thermal hydraulic phenomena with high heat transfer coefficient (HTC). Accordingly, various passive safety systems (PSSs), whose driving force is weaker than the active system, ensure their feasibility by utilizing the HTC of condensation. NuSacle SMR, a representative integrated pressurized water reactor (IPWR) type SMR, was designed with a fully passive safety design concept with the emergency core cooling system (ECCS) and the decay heat removal system (DHRS) [1]. Both of the PSSs use condensation as a major heat transfer mechanism. Other recent SMR designs such as the i-SMR [2], and AP-300 [3] also adopted condensation for their PSSs.

The need for numerical analysis increases as various designs of reactors and PSSs are proposed and developed. Many of previous analyses for recent SMRs have been conducted using numerical analysis tools such as RELAP5, MARS-KS, MELCOR, and SPACE [2, 4, 5]. The significant advantages of using the numerical tools such as low cost and time consumption, made them a powerful tool for predicting and evaluating performance of the thermal hydraulic system. However, it implies that the system analysis codes need to be well validated to attain sufficient confidence level for their calculation results.

In conclusion, we need to continuously validate the performance of the numerical analysis tools to use them as a power tool for the development and evaluation of innovative designs of SMRs and their systems. In particular, the prediction of condensation heat transfer is important because it is one of the critical factors in cooling performance of PSSs.

This study aimed to expand the validation database for the SPACE code. Our experimental facility, designed to examine wall condensation heat transfer, was set as the reference system. We developed corresponding input models for both the SPACE and MARS-KS codes. By comparing results from SPACE, MARS-KS, and experimental data, we validated the SPACE code's filmwise wall condensation heat transfer prediction performance.

2. Experimental setup

The test facility, shown in **Fig. 1**, designed for experiment of wall condensation heat transfer on a long vertical surface under low non-condensable gas (NCG) conditions. The facility comprises a closed-loop system that combines a water loop and a steam supply with a condensation section. Saturated steam from the steam generator (A) is routed to a header (B) and pressure-adjusted before entering the test section (C) where it condenses, with the resulting condensate collected in a tank (D). A vacuum pump (E) sets the initial pressure to control NCG levels, while a circulating water loop, driven by a centrifugal pump (H), cools the specimen; a heat exchanger (G) then maintains the coolant's subcooling as temperatures rise.

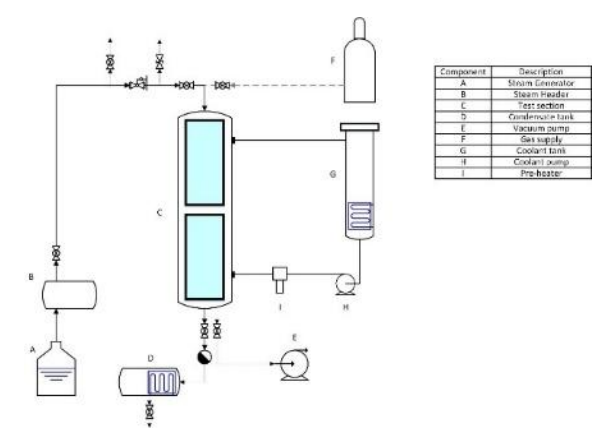


Figure 1. Test facility schematic.

Fig. 2 presents the test section, which is composed of a steam chamber, an aluminum test specimen (Al 6061), and a coolant channel that uses deionized water for condensation heat transfer. One side of the specimen is bonded to the coolant channel, while the other side is exposed to the steam inside the chamber. The chamber itself is a rectangular enclosure with a cross-sectional area of 134×184 mm² and a length of 1.1 m (excluding its inlet and outlet), and one of its side walls is left open

to serve as the condensing surface. By placing the specimen between the chamber and the coolant channel, one side directly contacts the steam, and the other side is directly cooled by coolant. The effective condensing area measures 100×1000 mm², and the specimen is 13 mm thick. Both the steam chamber and the coolant channel are fabricated from stainless steel (SS304).

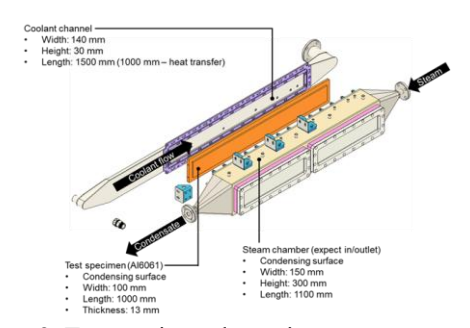


Figure 2. Test section schematic.

To determine the condensation heat flux, we computed both local heat flux and calorimetric heat flux using temperature data from the test specimen and cooling channel. Several TCs (thermocouples) and RTDs (resistance temperature detectors) were installed to monitor the test specimen and coolant temperature change. Measurements were taken at six axial positions along the condensing surface, 25, 75, 175, 335, 575, and 815 mm from the top as shown in Fig. 3. The RTDs captured the coolant and steam temperatures. The TCs were inserted into the test specimen. Three TCs were positioned parallel to the heat conduction direction at each of the measuring points. Moreover, we predicted condensation heat flux using the Nusselt condensation model. The local heat flux, calorie metric heat flux and the Nusselt condensation model were then calculated based on the following equations (1), (2) and (3), respectively.

$$q_{local}^{\prime\prime} = \frac{k(T_1 - T_3)}{\Delta x} \tag{1}$$

$$q_{calorie}^{"} = \frac{\dot{m}_l c_p (\overline{T_{i+1}} - T_i)}{A} \tag{2}$$

$$q''_{local} = \frac{k(T_1 - T_3)}{\Delta x}$$
(1)
$$q''_{calorie} = \frac{\dot{m}_l c_p(T_{i+1} - T_i)}{A_o}$$
(2)
$$q''_{Nusselt} = 0.943(T_{steam} - T_s) \left(\frac{\rho_l \Delta \rho g h_{fg} k_l^3}{\mu_l L(T_{sat} - T_s)}\right)^{1/4}$$
(3)

Where the k is thermal conductivity of the test specimen material (Al 6061), T_1 is the temperature measured by a TC closest to the condensing wall between the three TCs of a measurement point, T_3 is the temperature from the third TC, Δx is the distance between the first TC and the third TC, \dot{m}_l is the mass flow rate of the coolant, c_p is the specific heat of the coolant, T_i is the measured coolant temperature of the ith measure point, A_0 is the heat transfer area in the coolant channel, ρ_l is density of saturated water, $\Delta \rho$ is difference between the saturated water and steam, g is gravity acceleration, h_{fg} is evaporation heat of the saturated water, k_l is thermal conductivity of the water, μ_l is dynamic viscosity of the water, L is the distance of the temperature measurement point from the top of the condensation surface, T_{sat} is saturation temperature of the steam, T_s is temperature of the surface, and T_{steam} is the temperature of the steam.

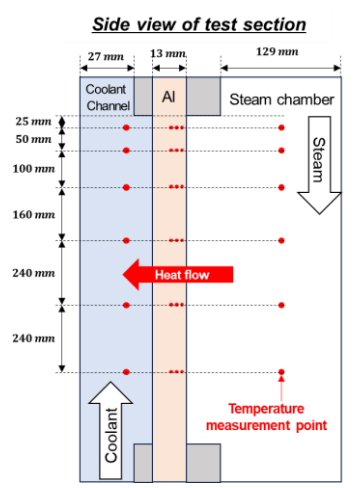


Figure 3. Schematic of temperature measurement points.

During the condensation experiment, the system was operated at an absolute pressure of 2.25 bar. The inlet temperature of the coolant in the cooling loop ranged from 60 °C to 65 °C, and the coolant mass flow rate was measured as 3.7 m³/hr using a turbine flow meter. At the start of each test, the steam chamber was evacuated using a vacuum pump until the pressure reading reached 0.04

3. Development of numerical analysis input model

For the numerical analysis of the condensation heat transfer, input model of the aforementioned test facility was developed for both SPACE and MARS-KS code. As thermal hydraulic system analysis codes for nuclear power plants, the SPACE and MARS-KS code mostly share input requirements. Accordingly, we could set most of the input data for the numerical analysis to be identical. Nodalization of the test facility was shown in Fig. 4.

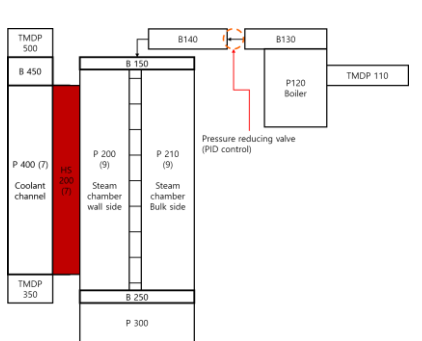


Figure 4. Nodalization of input model

The input model modeled major components of the test facility such as steam chamber, condensation surface, cooling channel, and boiler. Steam generation from the boiler was modeled by imposing heat source to the heater heat structure in the boiler. The steam chamber was modeled with two pipe components. One acts as bulk side volume and the other acts as wall side volume. Initial condition of each component was set to be 4.0 kPa dry air. The inlet and outlet of the coolant channel were set as flow boundary condition and pressure boundary condition, respectively. Flow rate and temperature of the coolant inlet boundary was referenced from the experimental condition.

Unlike MARS-KS code, SPACE code has options for users to choose models for condensation on a heat structure. Basic model is Colburn-Hougen model, which is used in MARS-KS code. Other options include No-Park model, and Vierow-Schrock model. In this study, we also compared the results attained from SPACE code using the condensation model options.

4. Results and discussions

We conducted eleven experimental tries and attained a series of wall condensation heat transfer datasets with calculated heat flux. The calculated heat flux means local heat flux and average heat flux at intervals between the measurement points. The heat flux data and predicted heat flux using Nusselt film condensation model was presented on Fig. 5. The local heat flux data ranged from 80 to 120 kW/m² while the calorimetric heat flux data ranged from 50 to 400 kW/m². We presumed that the discrepancy at the upper section resulted from the short interval between the measurement points. The short interval may imply insufficient mixing of the coolant, overestimating the coolant temperature difference. To simply validate the data, we calculated the expected heat flux using the Nusselt model. In this case, required variables such as pressure, surface and steam temperature were attained from the experimental measurements. As a result, the expected heat flux, ranging from 110 to 175 kW/m², showed high similarity with the local heat flux data. Accordingly, further comparison with the numerical calculation results was conducted with the local heat flux data from the experiment. Interestingly, condensation heat flux at the lower part of the specimen showed slight increase in every case and measurement. We presume that the relatively low temperature of the coolant inlet increased subcooling of the condensation surface, increasing the heat transfer. This trend can also be found in the Nusselt heat flux prediction which is affected by surface temperature.

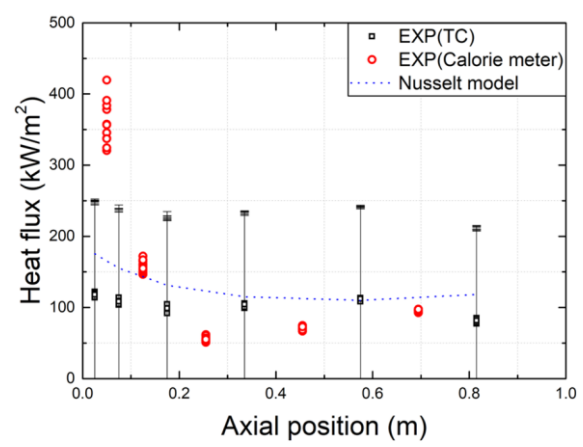


Figure 5. Axial heat flux data from wall condensation heat transfer experiments

Fig. 6 shows the results from SPACE and MARS-KS calculations with the experimental data. OPT0 stands for Colburn-Hougen model, which is default condensation heat transfer model. As option models for condensation heat transfer of the SPACE code, OPT1 and OPT2 mean No-Park model and Vierow-Shrock model, respectively. The MARS-KS code showed the data range from 42 to 64 kW/m² and the SPACE code with default option showed heat flux from 36 to 39 kW/m². Both data were notably lower than the heat flux data from the experiment. Also, the feature that the experimental data showed, slight increase of the heat flux at the lower section, was not observed. Still the MARS-KS showed decreasing heat flux at the top of the plate, which is similar trend with the experiment, while the SPACE did not. Considering that both cases used same condensation heat transfer model, we predicted that other thermal hydraulic variables such as NCG fraction and velocity of the steam have affected the condensation heat transfer. The condensation model showed differences between each other. The result with No-Park model showed much lower heat flux, ranging from 7 to 31 kW/m², while the Vierow-Schrock model showed much closer heat flux data to the experiment, ranging from 70 to 95 kW/m².

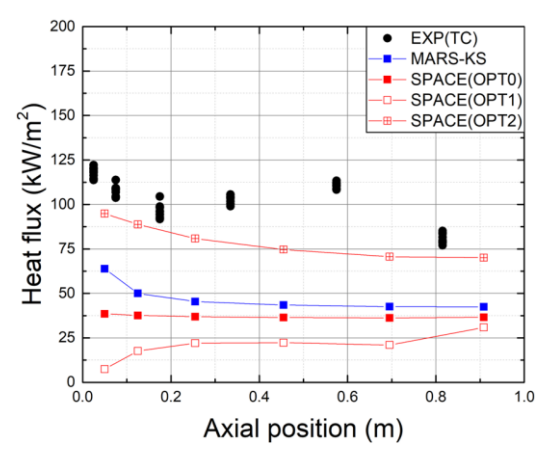


Figure 6. Axial heat flux data from the MARS-KS, SPACE, and experiments

As shown in **Fig. 7**, the axial NCG concentration distribution varied with the code. The MARS-KS showed relatively lower NCG concentration than the SPACE code. which is expected to be the reason for the discrepancy between the results from MARS-KS and SPACE with default option.

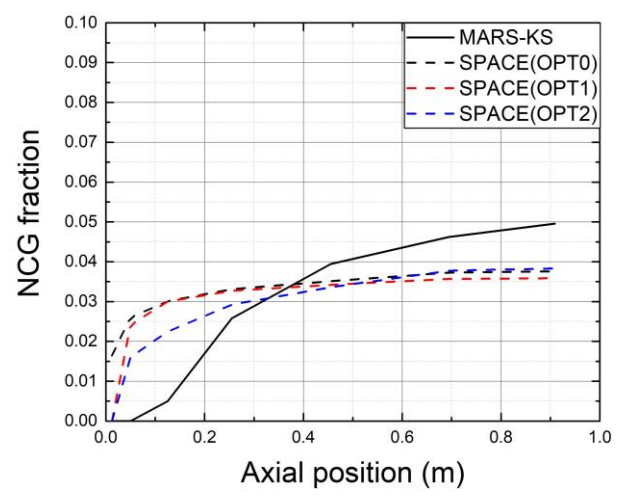


Figure 7. Axial NCG concentration from numerical analysis

The total heat transfer through the condensation surface was calculated as shown in Fig 8. The SPACE calculation result using the Vierow-Shrock condensation model showed the least error with the experiment while the SPACE result with the No-Park model showed the most error. The data from the MARS-KS and SPACE using same Colburn-Hougen model showed similar amount of error. The overall error of the numerical data can be expressed as presented in Fig 9. The prediction data from the SPACE code with Vierow-Shrock model laid within 40% error region while the other results were located out of the region.

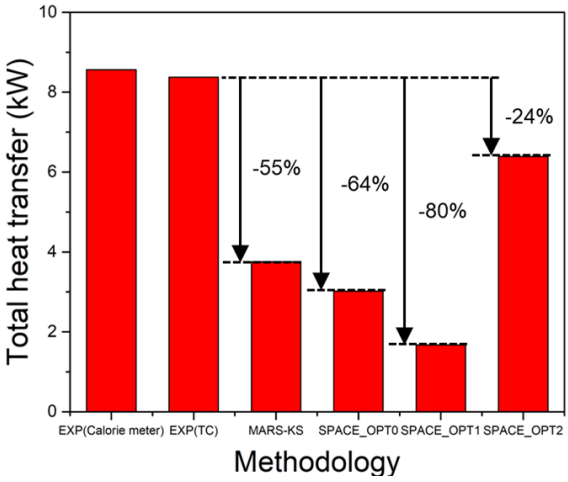


Figure 8. Total transferred heat at each methodology

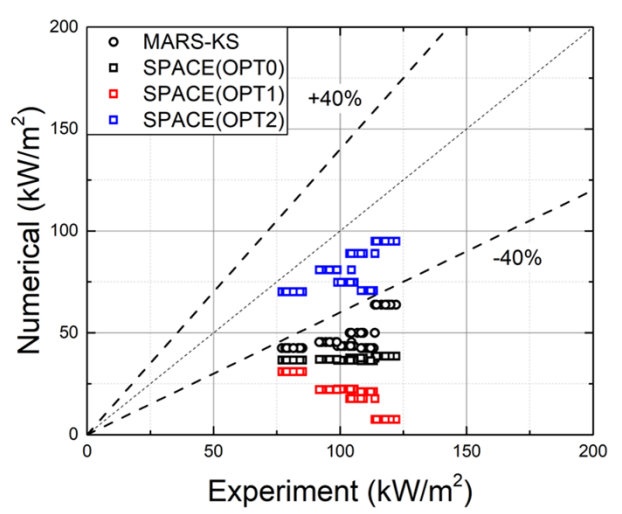


Figure 9. Error of numerical prediction compared to the experimental data

5. Conclusion

In this study, we constructed input models of a condensation heat transfer test facility for MARS-KS and SPACE code to validate the condensation heat transfer prediction performance of the codes. We compared the experimental data with the numerical calculation results. Moreover, we considered the sensitivity of the condensation model options that the SPACE code provides. The results showed that the SPACE code with Vierow-Shrock model, which is optional condensation heat transfer model, showed the closest results to the experimental data. On the other hands, results from the No-Park model showed significant discrepancy with experiment. The results from MARS-KS code and SPACE with Colburn-Hougen showed intermediate prediction performance but still showed notable difference with the experiment. Accordingly, we need to consider optional condensation heat transfer models and conduct sensitivity analysis about the options.

Acknowledgments

This work was supported by the Nuclear Safety Research Program through the Regulatory Research Management Agency for SMRs (RMAS) and the Nuclear Safety and Security Commission (NSSC) of the Republic of Korea. (RS-2025-02311026), and also was supported by the National Research Foundation of Korea (NRF) grant funded by the Korean government (MSIT) (No. RS-2022-NR067165)

REFERENCES

- [1] NUSCALE, NuScale Plant Design Overview, NuScale Power: Corvalis, Oregon (2014).
- [2] Chang Hyun Song, et al. Evaluation of accident mitigation capability of passive core and containment cooling system of i-SMR under representative LOCA and non-LOCA

conditions, Nuclear Engineering and Technology, 57.8 (2025) 103556

- [3] AP300 SMR. 2025. Available online:
- https://westinghousenuclear.com/energy-systems/ap300-smr/ (accessed on 17 March 2025).
- [4] Hyo Jun An, et al. Strategic analysis on sizing of flooding valve for successful accident management of small modular reactor, Nuclear Engineering and Technology, 56 (2024) 949-958.
- [5] Michael Gorman, et al. TRACE system code benchmark of Station Blackout of a NuScale-like reactor and comparison with NuScale simulator, Annals of Nuclear Energy, 213 (2025) 111078.